91602
new 82-10

ontario hydro
research division

COMPLIMENTARY COPY
Please Credit Ontario Hydro Research if
Reproduced in Whole or in Part

EVALUATION OF CEMENT-BASED BACKFILL MATERIALS

Report No. 87-223-K

R. Dayal
Senior Geochemist
and
R. Klein
Hydrogeology Technician
Rock Sciences Section
Civil Research Department

ABSTRACT

Work has been in progress at Ontario Hydro to develop and evaluate potential backfill materials for use in a reactor waste repository. A carbonation and gas permeability test cell has been set up to evaluate gaseous CO_2/grout interactions and their effect on material properties. This report presents a preliminary geochemical evaluation of one grout mix developed at Ontario Hydro, with particular reference to the carbonation and gas permeability tests, carbonation-induced changes in material properties, and the effects of carbonation on radionuclide transport and water ingress properties.

job	file	date	report no.
44-314-062 44-122-460	841.2	September 29, 1987	87-223-K

TABLE OF CONTENTS

		Page
1.0	INTRODUCTION	1
2.0	BACKFILL MATERIAL SELECTION AND PERFORMANCE REQUIREMENTS	1
3.0	RESULTS AND DISCUSSION	3
3.1	Carbonation and Gas Permeability Tests	3
3.2	Carbonation-Induced Changes in Material Characteristics	10
3.3	Carbonation Mechanisms and C-14 Mobility	39
3.4	Effects of Carbonation on Radionuclide Attenuation and Water Ingress Properties	40
4.0	CONCLUSIONS	43
5.0	ACKNOWLEDGEMENTS	44
REFERENCES		45
DISTRIBUTION		last page

ontario hydro
research division

To Mr. H.N. Isaac, Manager
Nuclear Materials Management Dept
Design and Development Division

Attn: Dr. S. Naqvi/Mr. P.K.M. Rao

EVALUATION OF CEMENT-BASED BACKFILL MATERIALS

1.0 INTRODUCTION

Although the current strategy at Ontario Hydro calls for extended storage of reactor wastes at Ontario Hydro's Bruce Nuclear Power Development Site, various concepts for the disposal of these wastes have been considered and evaluated in the past. Depending upon site and waste characteristics, the Ontario Hydro disposal options have included: (a) engineered trenches and tunnels or augered boreholes in glacial till at shallow depths, and (b) mined caverns in shale or limestone at shallow to intermediate depths. All of these design options will require engineered enhancements to provide trench stability, as well as to reduce water ingress and radionuclide migration. Of particular importance for effective isolation of radioactive waste, especially that containing C-14, is the need for proper backfilling and sealing of the disposal facility.

With these considerations in mind, work has been in progress at Ontario Hydro to develop and evaluate potential backfilling materials for a reactor waste repository. The main objective of this research project is to develop an adequate data base for performance evaluation of candidate backfill materials, in particular, cement-based grouts and concretes developed at Ontario Hydro.

2.0 BACKFILL MATERIAL SELECTION AND PERFORMANCE REQUIREMENTS

Some of the important functions of backfill in a reactor waste repository are to: (a) fill and seal the emplacement hole including the inaccessible void space between waste packages; (b) reduce or control ingress of infiltrating water; (c) provide trench stability and minimize subsidence; (d) attenuate radionuclide migration by impeding water movement; and (e) serve as an effective geochemical sink for radionuclides, in particular, C-14.

For this project, existing grout and concrete formulations developed at Ontario Hydro are being evaluated (Dayal, 1986a). In this preliminary study, two cement-based grouts and a cement-fly ash concrete mix, all containing

varying amounts of fluidizing and/or expanding admixtures, were selected for geochemical evaluation (Table 1). An important aspect of backfill material development is to assess the use of fly ash and other supplementary materials as a substitute for cement in order to keep the material costs minimal.

An important criterion for the backfill to serve as an effective barrier is its ability to control inflow of infiltrating rainwater into the repository. Controlling the rate of water ingress will not only protect the waste package from degradation but also minimize waste form leaching and impede radionuclide transport by reduced water movement.

A simple leaching experiment illustrates the effect of water flow rate on waste form leaching and radionuclide release rates (Dayal, 1986b). Leaching data for cemented ion exchange resin waste, based on the modified IAEA test, indicate that both Cs-137 and Sr-85 exhibit a distinct trend of decreasing rates of release with decreasing frequency of leachant renewal. The observed decrease in leach rate with increasing leachant residence time can be attributed to saturation effects resulting from build-up of dissolution products in the leachate. However, at low or zero flow rates, such as that represented by the static leach test, the leachant is reasonably stagnant for sufficiently long periods of time so that the overall release becomes diffusion-controlled. At slightly higher flow rates, it is the rate of transport of dissolution products away from the water form/water interface which becomes rate-controlling. In this case, it is the rate of water flow past the solid waste that limits radionuclide release.

Table 1. Material Compositions and Mix Proportions

	Test Materials (Mix No.)		
Mix Proportion[a]	Cement Grout (13711)	Cement/Fly Ash Grout (13715)	Cement/Fly Ash Concrete[b]
Cement	21.1	16.9	285
Sand	31.7	31.7	1920
Water	8.5	6.8	144 - 158
Fly Ash	--	4.2	70
Admixture[a]			
Intrusion Aid	0.21	0.21	--
Melmet	--	--	c
Water/Cement Ratio	0.40	0.40	0.50 - 0.55

a All values are given in Kg.
b Further details are given in Deans (1984).
c 1.0 to 2.0% of cementing material.

High rates of advective transport will tend to increase the concentration gradients at waste form/leachant interface, thereby increasing the rates of radionuclide release.

It is clear from the above discussion that groundwater availability or ingress is an important factor in determining release of radionuclides. Therefore, engineered barriers can be used to control water ingress which, in turn, will minimize radionuclide release to the extent where diffusion becomes rate-controlling.

Another important part of backfill material development and optimization is the requirement that backfill serve as an effective geochemical barrier to migration of radionuclides escaping from the waste package. The candidate materials should have the ability to attenuate and contain waste radionuclides for time periods commensurate with their radioactive half-lives.

The predominant radionuclides in CANDU reactor waste are H-3, C-14, Cs-137, and Co-60. Of particular importance is C-14 because of its long half-life and correspondingly longer term isolation. A major part of C-14 generated is associated with moderator ion exchange resin in the form of carbonate and bicarbonate. Since both carbonate and bicarbonate are known to be relatively mobile in soil and rock media, work was initiated at Ontario Hydro Research, in conjunction with the University of Waterloo (Reardon, 1986; Moddle et al., 1986) to develop and evaluate engineered barriers suitable for C-14 attenuation and containment in a reactor waste repository.

3.0 RESULTS AND DISCUSSION

Preliminary geochemical work initiated at Ontario Hydro has focussed on evaluation of gaseous CO_2/grout interactions and their effect on radiocarbon attenuation in a cementitious matrix. One management option being considered for concentrated C-14 wastes is deep geologic disposal. Although it is unlikely that C-14 would be present as gaseous $^{14}CO_2$ in a repository environment at depth, preliminary results of our laboratory study involving gaseous CO_2 as a reactant do provide useful information on the nature of carbonation and the character of carbonated reaction products, and their effect on subsequent radionuclide reactivity and attenuation. In particular, a discussion of carbonation-induced changes in material characteristics with particular reference to the effects of carbonation on radionuclide attenuation and water ingress properties is presented.

3.1 Carbonation and Gas Permeability Tests

A gas permeability test for concrete reported recently by Martin (1986) has been modified in our laboratory for studying gaseous carbon dioxide reactivity in cementitious backfill materials. The modification involved incorporation of humidity and temperature probes in the test cell to monitor changes in these parameters with time. An attractive feature of the test method is its versatility in allowing both nitrogen and carbon dioxide to be used

sequentially in a repetitive mode, so that the effects of induced carbonation on gas permeability can be evaluated. An added benefit of the modified test method is that it can be used in a vacuum mode to estimate air permeabilities using the radial air withdrawal transient vacuum technique (Loughborough, 1966; Jakubick and Klein, 1986).

The cylindrical test specimen (nominal size: 15 x 15, diameter x height, cm), with a 3.3 cm-diameter hole drilled in the centre, is held tightly between two end plates (Fig. 1). To eliminate any gas leakage in the system, an effective seal was obtained by using rubberized cork gasket between the specimen and each plate.

As shown in the schematic in Fig. 2, the assembled test specimen was connected to a gas reservoir (1.0 litre capacity) fitted with a pressure gauge, a high precision transducer, and a manual gas inlet valve. The reservoir was filled with gas from a tank and the initial pressure was set at 150 psi. Based on a series of trials at different start pressures, Martin (1986) established that 150 psi was a reasonable start pressure for the tests because a higher pressure could have caused too high a tensile strength in the specimen, resulting in cracking or failure. A multi-channel datalogger was connected to the pressure transducer and temperature and humidity probes to record changes in these parameters. An on-line computer controlled the datalogger, with the data being stored on a floppy disc. A photograph of the carbonation and gas permeability testing system is shown in Fig. 3.

The test was initiated by applying a gas pressure of 150 psi to the assembled rig, thereby axially injecting nitrogen or carbon dioxide into the test specimen and, in the process, inducing radial gas flow through the medium. All tests were conducted at ambient laboratory temperature on grout specimens dried at 40°C for an extended time period until no further change in mass was observed. Temperature variation in the laboratory during a typical test run was found to be too small to significantly affect the gas pressure in the reservoir.

The test programme involved measurement of the relative permeabilities of test material by passing sequentially inert nitrogen and reactive carbon dioxide through it. The changes in pressure, humidity, and temperature, both outside and within the test specimen were continuously recorded during the test run. The rate of drop in nitrogen pressure with time in the test specimen was used as a measure of relative gas permeability.

In the first test, grout (mix no 13711) test specimen was subjected to a series of repeat tests using nitrogen and carbon dioxide in the sequence given in Table 1.

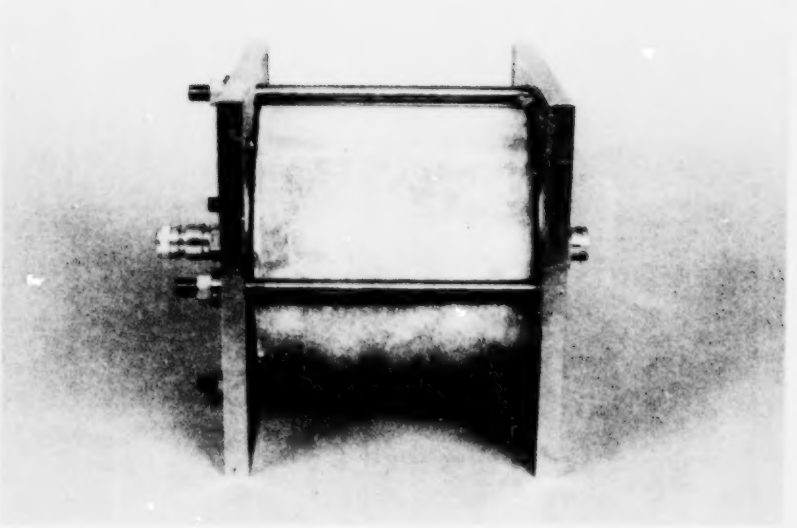

Figure 1. The assembled test rig with the cylindrical grout specimen.

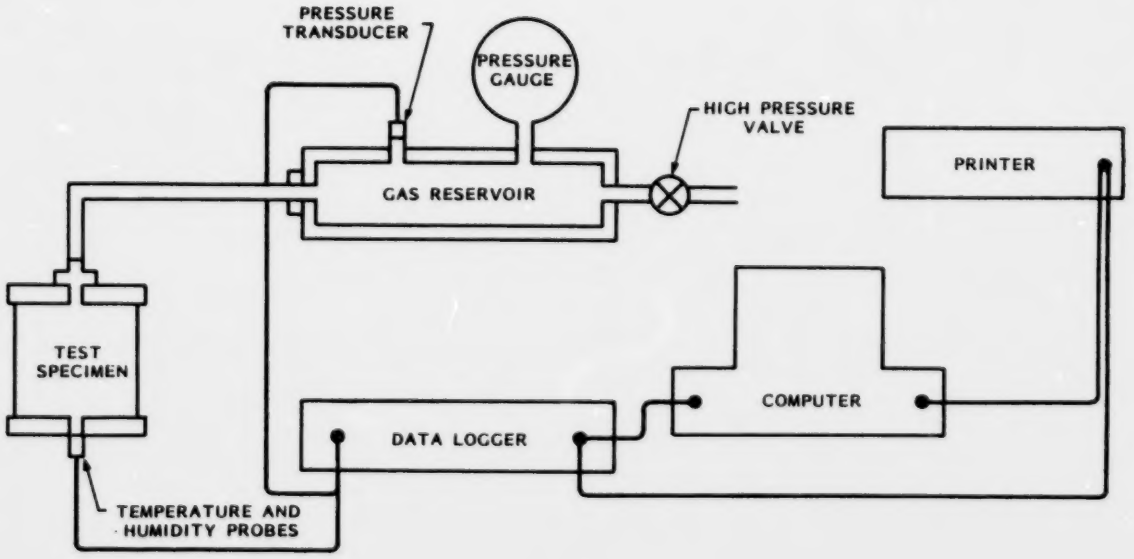

Figure 2. A schematic of carbonation and gas permeability testing system.

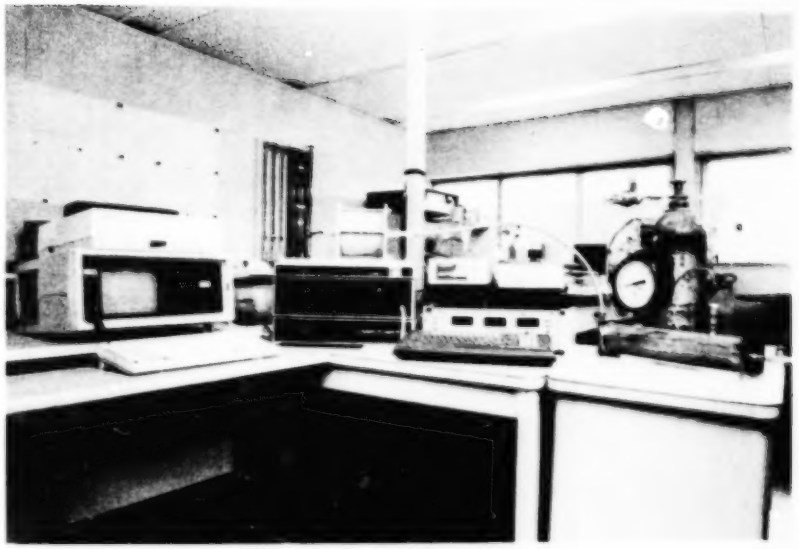

Figure 3. Experimental set-up for carbonation and gas permeability test.

Table 1. Sequence of Nitrogen and Carbon Dioxide Repeat Tests[a]

Sequence	Nitrogen Test	Carbonation Test
Nitrogen	N-1	---
Carbon Dioxide	---	C-1
Nitrogen[b]	N-2[c]	---
Nitrogen[b]		
Carbon Dioxide	---	C-2
Nitrogen[b]	N-3[c]	---
Nitrogen[b]		
Carbon Dioxide	---	C-3
Carbon Dioxide	---	C-4
Nitrogen	N-4	---

a Performed on grout specimen #13711.
b Following the first and second carbonation tests, repeat tests were performed using nitrogen to determine the reproducibility of the permeability measurements. The results show that the repeat curves are fairly close to the original curves, indicating good reproducibility.
c Represent mean of two nitrogen runs in each case.

Relative to nitrogen permeability, tests with CO_2 exhibit a significant drop in permeability as a result of carbonation. A further reduction in permeability is observed when the test specimen is subjected to successive carbonation cycles. Reduction in permeability following carbonation of concrete is well-known and reported in concrete and civil engineering literature.

Replotting the permeability data as log P versus time (t) indicates that the nitrogen curves approximate a linear relationship reflecting exponential gas decay with time and represented by:

$$\log P = 1 - mt \qquad (1)$$

where m is a constant and characteristic of material permeability. However, a close examination of the plots reveals that the nitrogen decay curves do not completely follow an exponential relationship (Fig. 4). The observed discontinuities reflect an initially rapid drop in pressure, followed by a more gradual rate of pressure drop over a longer time period. It is quite plausible that the initial, rapid pressure drop may be a result of the mobilization and transport, in a radial direction, of entrapped moisture from the interior of the test specimen (close to the cavity) towards the exterior (at a distance from the cavity), where it apparently builds up and serves to restrict the flow of gas, thus resulting subsequently in a slightly lower rate of pressure drop with time. Disregarding the initial transient, the nitrogen decay curves for longer time periods are assumed to characterize bulk material permeability.

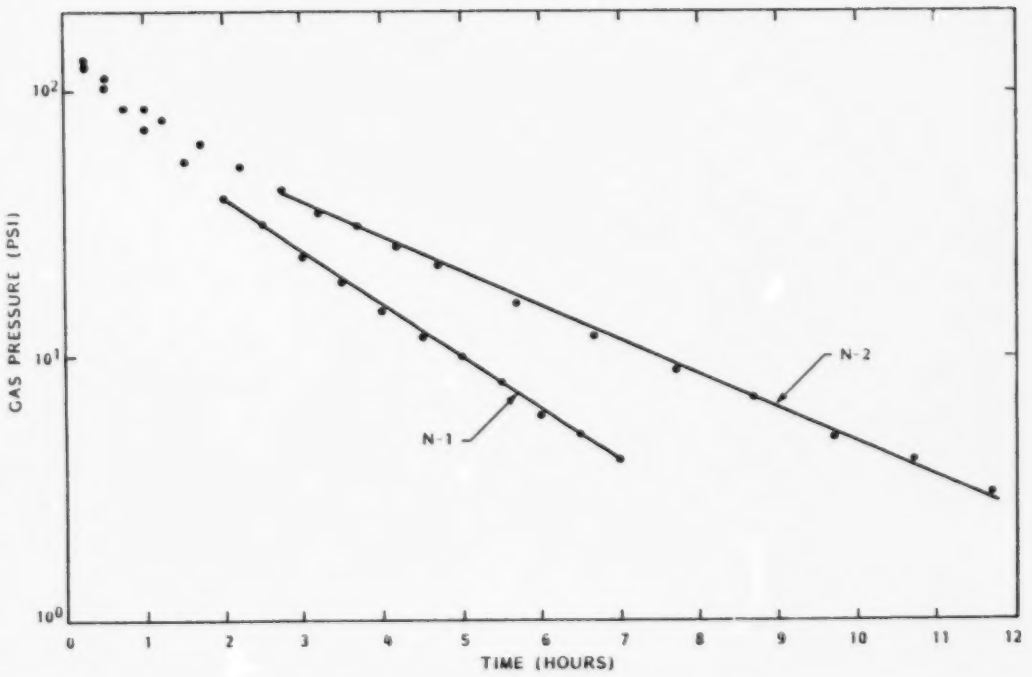

Figure 4. Nitrogen gas pressure drop with time, showing an exponential decay relationship over longer time periods.

The CO_2 plots, on the other hand, deviate from linearity, indicating that, unlike N_2, CO_2 does not follow a simple exponential decay relationship with time. This is not surprising considering that CO_2 is highly reactive with cement-based materials and that the induced carbonation results in progressively decreasing permeability.

As evident from Figs. 5 and 6, the CO_2 curves C-1 and C-2, compared to the corresponding nitrogen curves N-1 and N-2, exhibit a much faster drop in pressure with time, reflecting not only the effectiveness of grout as a sink for CO_2 but also total consumption of CO_2 in the carbonation process. In the third carbonation test, the curve C-3 indicates initial, rapid CO_2 removal by grout, whereas the latter part of the curve reflects progressively decreasing permeability due to carbonation (Fig. 7). The effect of successive carbonations (C-3 and C-4) on grout permeability is evident from nitrogen curves N-3 and N-4, which represent nitrogen tests performed before and after two consecutive carbonation tests (Fig. 8).

3.2 Carbonation-Induced Changes in Material Characteristics

In order to determine the nature and spatial extent of carbonation induced in the test material, the carbonated specimen was cored and sectioned for analyses as follows.

Following the final carbonation cycle, the specimen was removed from the test rig and cut perpendicular to the cylindrical axis into three equal sections A, B, and C. As shown in Fig. 9, four cores (8.6mm diameter) were drilled radially in each section A and C. The cores were sectioned into 5mm increments, with section 1 representing the part adjacent to the specimen cavity and section 6 at the other end of the core. The core sections were analyzed by x-ray diffraction and infra-red analyses for identification of carbonation reaction products. Nitrogen gas adsorption BET method was used for the determination of reactive surface area and pore size distribution of both carbonated and non-carbonated material.

A thin-section was prepared from a radial section of slice A for microscopic examination of carbonated test material (Fig. 9). For comparison purposes, a thin-section was also prepared from uncarbonated material. Two 2.5 cm diameter cores were drilled radially into section B (Fig. 9) and cut into 1.25 cm sections, with section 1 representing the interior of the specimen. Porosity and permeability measurements were performed on the core samples using a helium porosimeter and an air permeability apparatus. The changes observed in test material properties following carbonation are discussed below.

3.2.1 Permeability and Porosity

The changes induced in material permeability and porosity as a result of carbonation are important because they directly affect the water ingress properties of backfill materials.

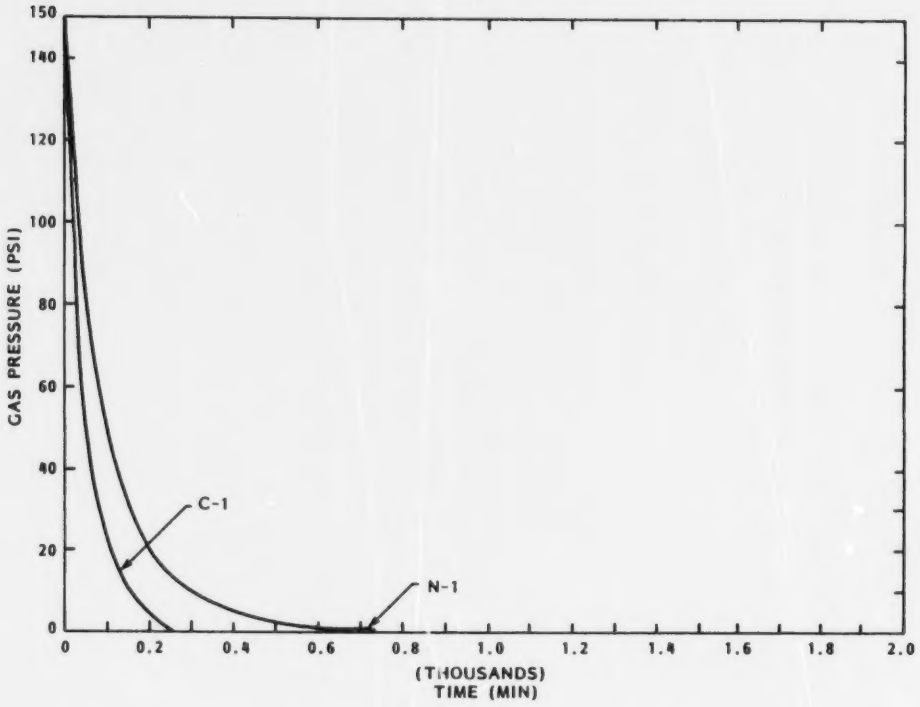

Figure 5. The first set of nitrogen (N-1) and carbon dioxide (C-1) permeability tests.

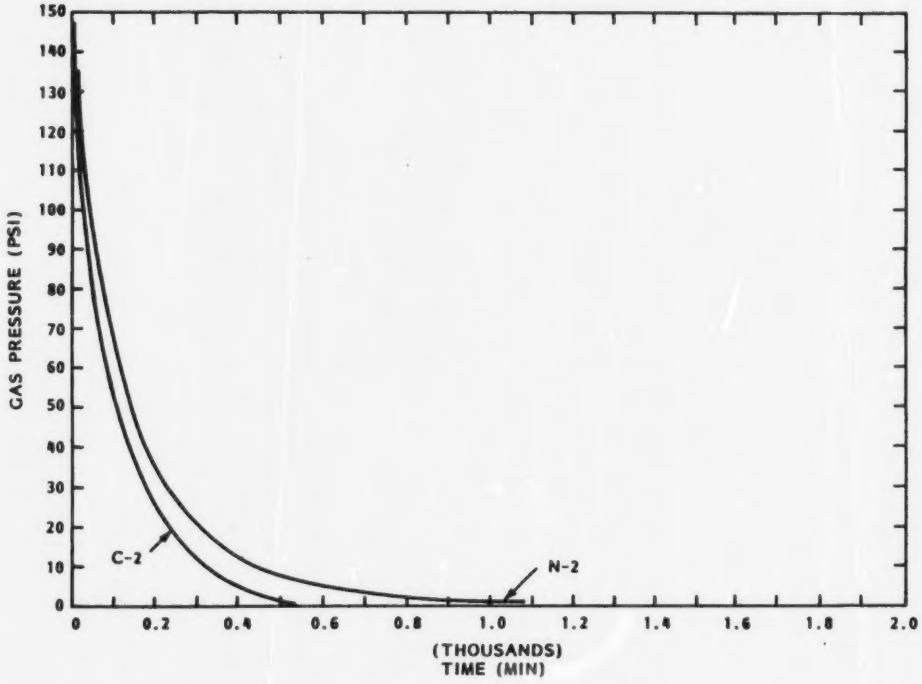

Figure 6. The second set of nitrogen (N-2) and carbon dioxide (C-2) permeability tests.

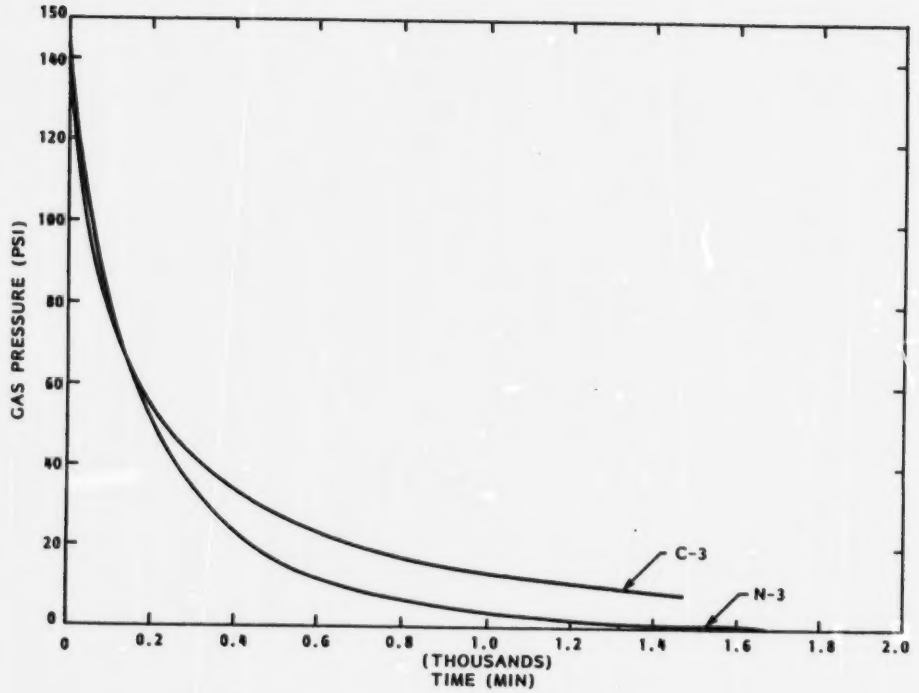

Figure 7. The third set of nitrogen (N-3) and carbon dioxide (C-3) permeability tests.

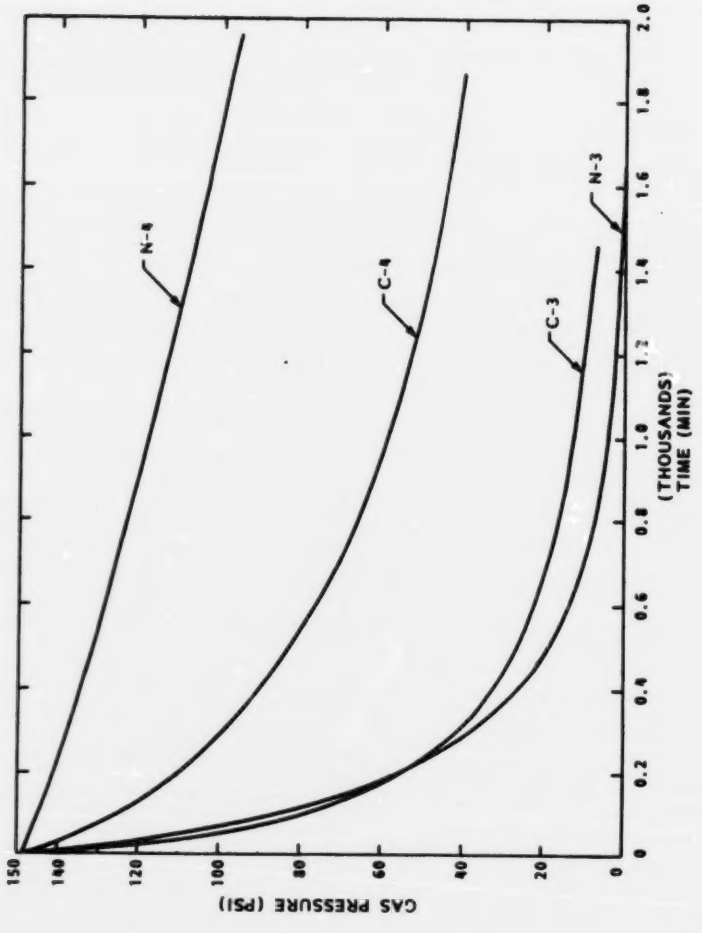

Figure 8. Effect of successive carbonations (C-3, C-4) on nitrogen permeabilities (N-3, N-4).

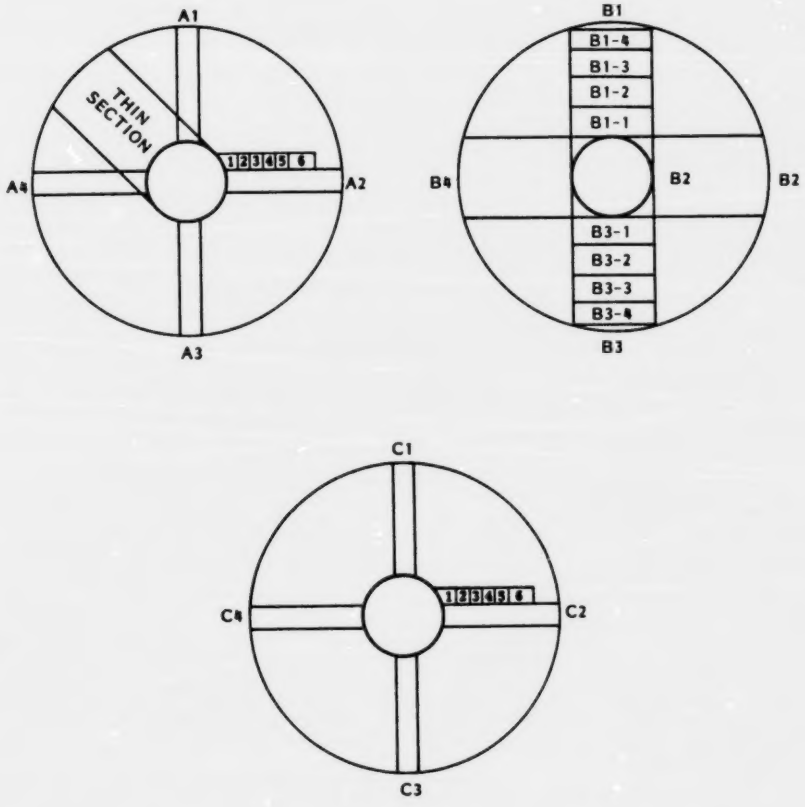

Figure 9. A cross-sectional view of radial drill cores taken from sections A, B and C of the carbonated test specimen.

The observed reduction in permeability as a result of successive carbonations is evident from log P versus time exponential decay curves based on a series of nitrogen tests conducted before and subsequent to the carbonation tests (Fig. 10). Using eq. (1), values for m, which represents a relative measure of material permeability, were calculated. As presented in Table 2, the values for m decrease progressively with increasing degree of carbonation resulting from successive carbonations. A comparison of the m values for N-1 and N-4 indicates a thirty-fold net reduction in permeability following the four carbonations. The sharpest drop in permeability is observed for N-4 (~15-fold), attributable to two successive carbonations following N-3.

It should be noted, however, that the observed reduction in permeability could also be related to the moisture content of the test specimen. Previous work has shown that gas permeability is reduced significantly with increasing moisture content of concrete (Loughborough, 1966; Figg, 1973; Jakubick and Klein, 1986). Moisture generated during carbonation reaction is reflected in the humidity probe readings during a carbonation run. The effect of the resultant moisture gradient in carbonated specimen on gas permeability is difficult to evaluate at this time.

Table 2. Relative Changes in Material Permeability Following Carbonation

Test	Permeability Index (λ_m)[a]
N-1	0.53
N-2	0.37
N-3	0.25
N-4	0.017

[a] Based on eq. (1), the units for m are psi/hour
[b] N-3 was followed by two successive carbonations, prior to N-4 test.

Permeability and porosity measurements performed on core-sections from carbonated test specimen to obtain information on the spatial extent of the carbonation front indicate a progressive reduction in both permeability and porosity from the exterior towards the interior, the most carbonated region of the test specimen (Figs. 11, 12). For example, the permeability and porosity values exhibit a systematic decrease from 132 μD and 22% for the least carbonated section of the core to 40 μD and 17% for the most carbonated part, adjacent to the specimen cavity. The observed permeability and porosity profiles cannot be attributed to varying moisture contents because all core sections were dried to constant weight prior to analysis.

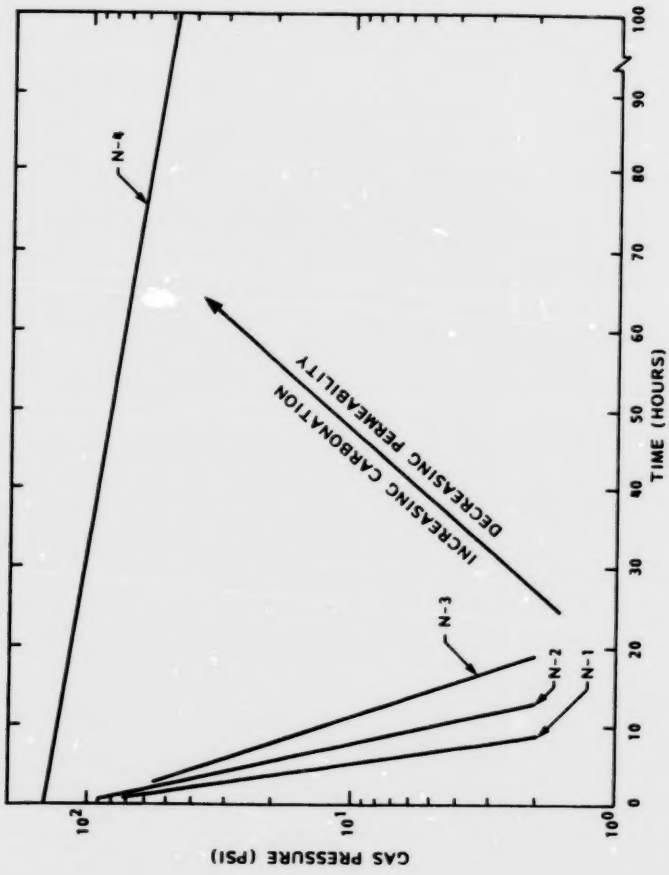

Figure 10. Decreasing material permeability with increasing degree of carbonation.

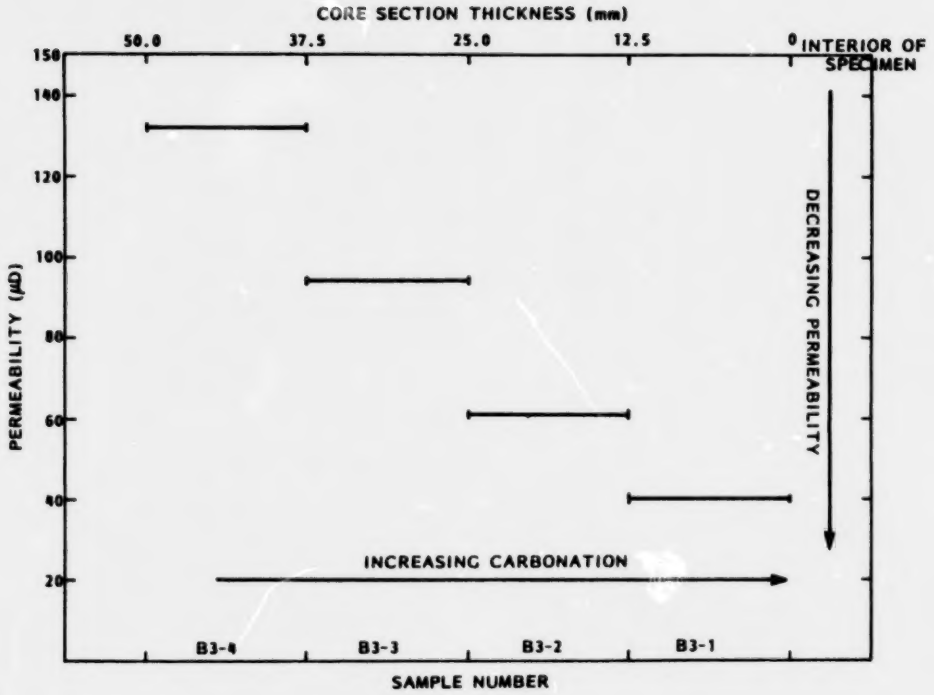

Figure 11. Decreasing permeability with increasing degree of carbonation of test material.

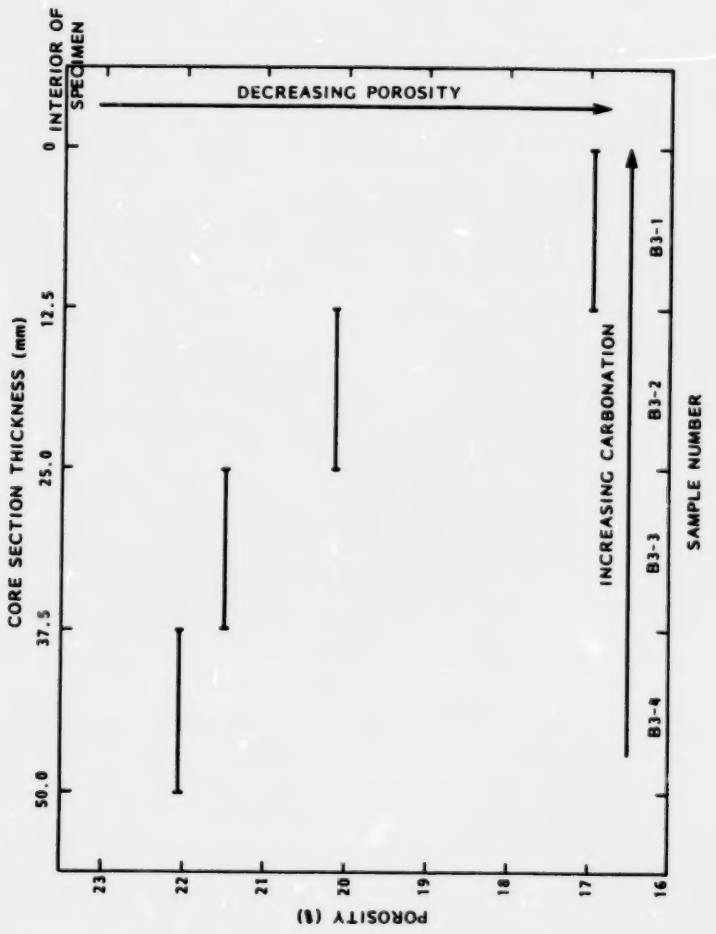

Figure 12. Decreasing porosity with increasing degree of carbonation of test material.

3.2.2 Reactive Surface Area and Pore Size Distribution

Specific surface area measurements made on core-sections of carbonated test specimen reveal that relative to the exterior of the specimen, the core-section adjacent to the specimen cavity and representing the most carbonated part of the specimen has a significantly higher specific surface area (Fig. 13). The most pronounced increase in specific surface area is observed for 0-5 cm section, the section adjacent to the specimen cavity. The depth profile of average pore radius with increasing distance towards the specimen interior is displayed in Fig. 14, which indicates a trend of decreasing pore size with increasing distance towards the specimen interior, representing increasing degree of carbonation with depth. As expected, the pore size distribution depth profile is an approximate mirror image of the specific surface area depth profile displayed in Fig. 13.

3.2.3 Radionuclide Attenuation

Radionuclide sorption tests were performed on core-sections of carbonated test material to evaluate the effect of carbonation, to varying degrees, on radionuclide attenuation. Preliminary results of Cs-137 sorption tests performed on intact disc specimens (26 x 2, diameter x thickness, mm) from carbonated test material are presented as sorption coefficients in terms of K_D and K_A (normalized to geometric surface area) values in Figs. 15 and 16, respectively. The data clearly show a trend of increasing cesium sorption with increasing extent of carbonation, most likely a reflection of higher reactivity of carbonated material as expressed by relatively higher specific surface areas in Fig. 13.

Preliminary tests to evaluate C-14 uptake behaviour indicate significantly lower $^{14}CO_3$ removal from solution by carbonated material, compared to that by non-carbonated materials.

Further tests to evaluate Cs-137 are C-14 sorption and diffusion behaviour in both carbonated and non-carbonated grout are in progress.

3.2.4 Phase and Textural Changes in Carbonated Material

X-ray diffraction, infra-red spectroscopy, and light microscopic techniques were employed to identify the carbonation-induced phase and textural changes in the test material. X-ray diffraction pattern of non-carbonated material shows the presence of portlandite as indicated by strong (001), (101), (102), and (110) peaks. However, upon carbonation, a progressive decrease in portlandite peak intensities, relative to quartz, is observed with increasing distance towards the specimen interior. Fig. 17 shows a complete absence of portlandite in core-section C2-1, representing the most carbonated part of the test specimen.

X-ray diffraction scans of test material in the 25-35° 2θ region show that, relative to quartz, both calcite and dolomite peaks exhibit significant enhancement in peak intensities for carbonated material (Fig. 18). As

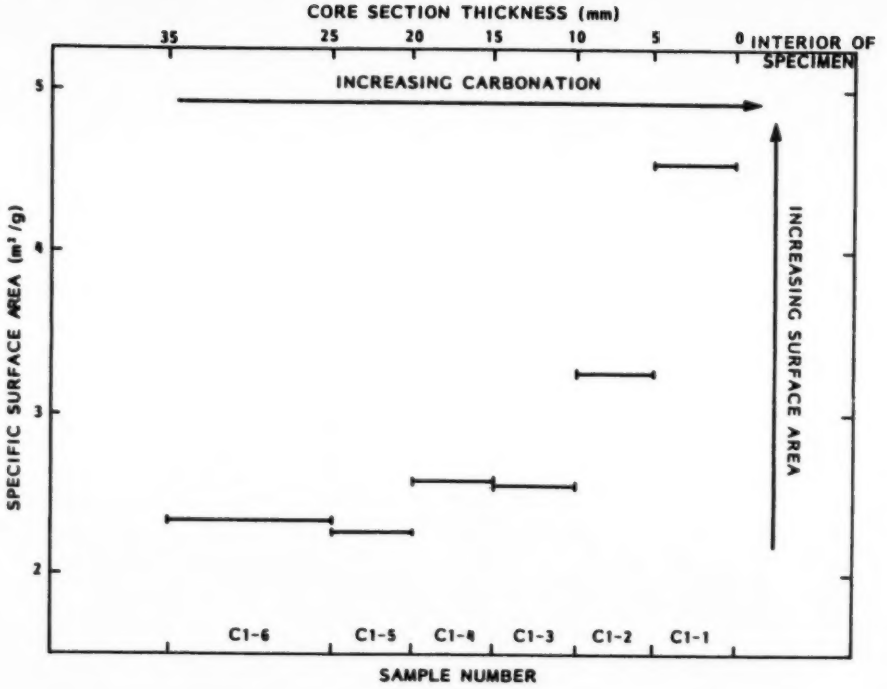

Figure 13. Increasing surface area with increasing degree of carbonation.

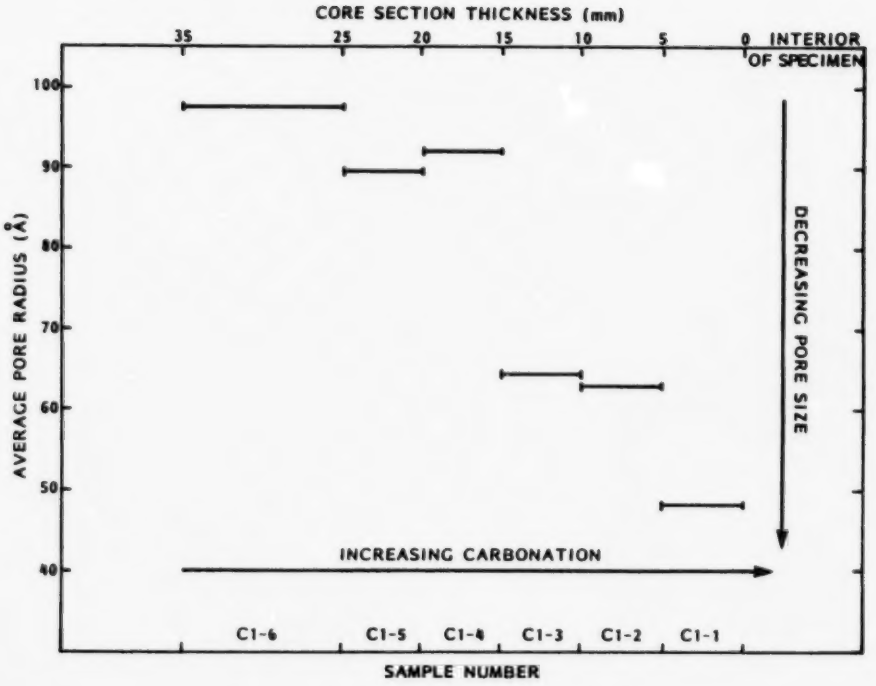

Figure 14. Decreasing pore size with increasing degree of carbonation.

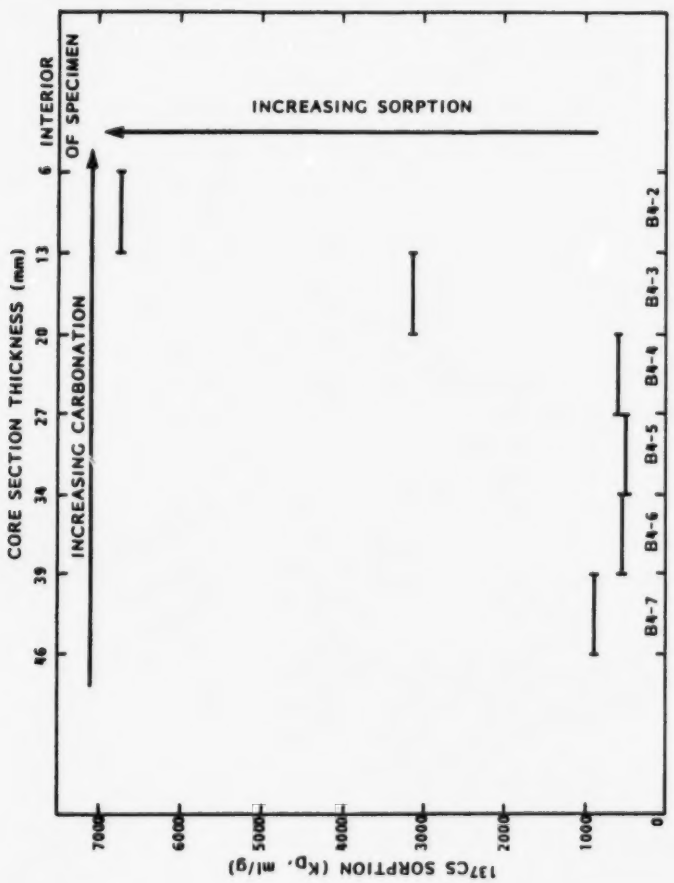

Figure 15. Increasing Cs-137 sorption expressed as K_D(mL/g) with increasing degree of carbonation.

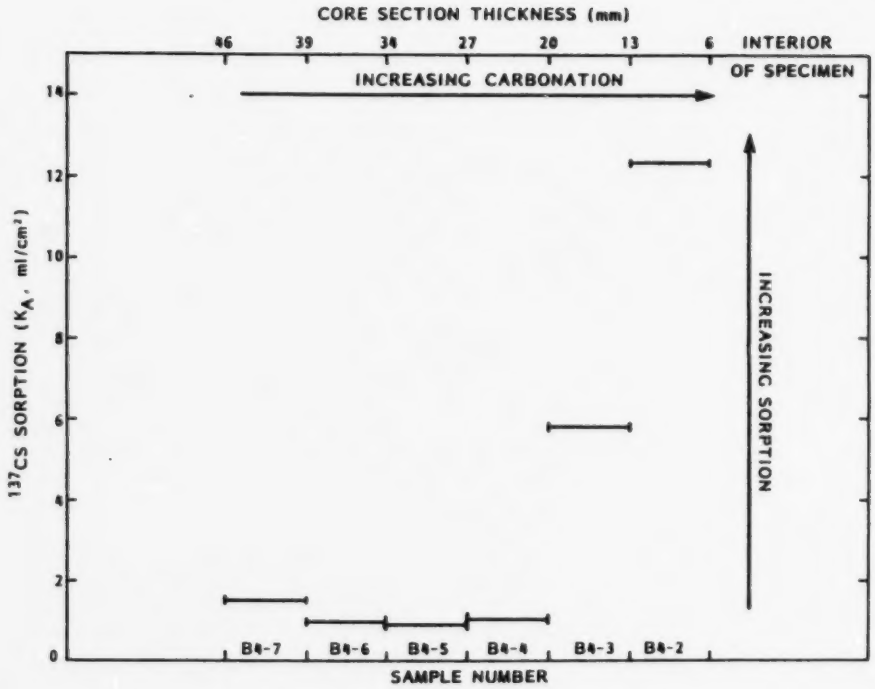

Figure 16. Increasing Cs-137 sorption expressed as K_A(mL/cm^2) with increasing degree of carbonation.

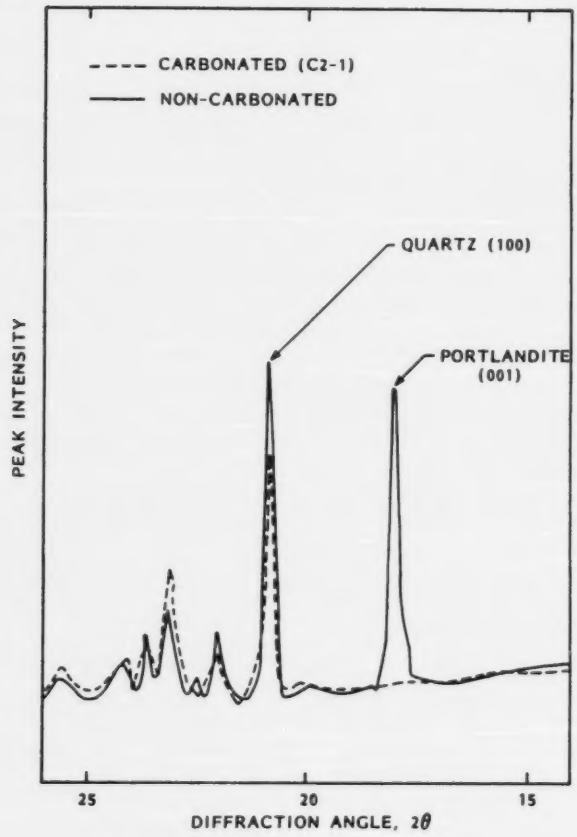

Figure 17. X-ray diffraction patterns of carbonated and non-carbonated test material, showing changes in relative peak intensity of portlandite.

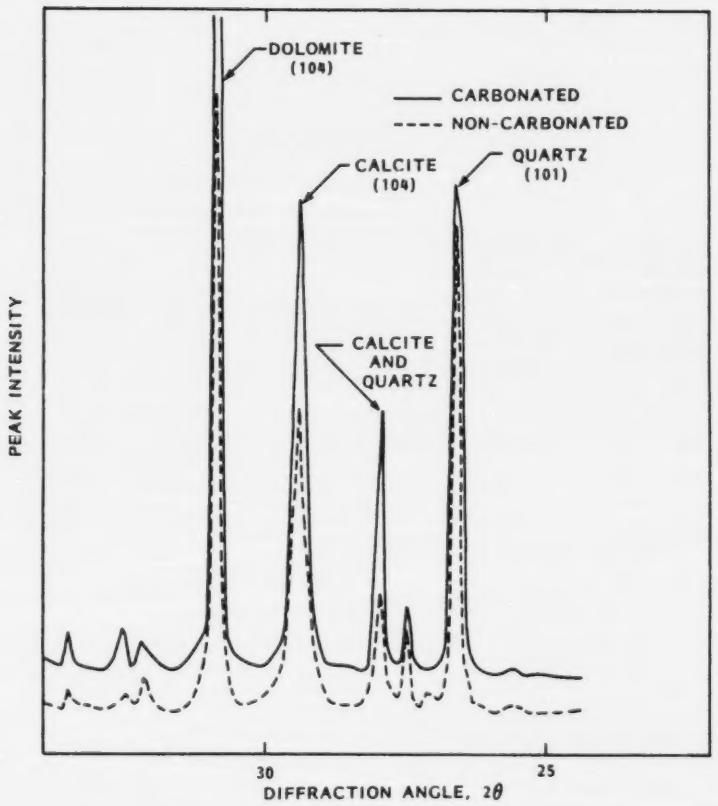

Figure 18. X-ray diffraction patterns of carbonated and non-carbonated test material, showing changes in relative peak intensities of calcite and dolomite.

indicated by the calcite (104)/quartz (101) peak intensity ratios in Fig. 19, calcite exhibits a progressive increase with increasing degree of carbonation towards the specimen interior.

Tobermorite, a calcium silicate hydrate and represented by a weak 11 Å peak, was found to be absent in carbonated material.

Infra-red spectra of the same materials show strong carbonate bands at 1450 and 880 cm^{-1} (Fig. 20). Based on x-ray diffraction data, the carbonate bands can be attributed to the presence of calcite, not vaterite or aragonite. In fact, the very intense band at 1450 cm^{-1} shows a progressive increase in intensity with increasing degree of material carbonation.

Besides the distinct absorption bands for carbonate, a sharp band is observed at ~ 3600 cm^{-1}, corresponding to calcium hydroxide in non-carbonated material. Upon carbonation, however, this band is absent as evident from Fig. 18.

Fig. 18 also reveals the relative changes in the absorption bands at 1100 cm^{-1} for silica gel and at 1000 cm^{-1} for calcium silicate hydrate. Following carbonation, the calcium silicate hydrate band intensity is significantly reduced with a corresponding increase in the absorption band intensity for silica gel, indicating that calcium silicate hydrate is transformed to silica gel during the carbonation process.

In order to determine mineralogical and textural changes induced in the grout material as a result of carbonation, a 30 x 65 mm thin-section was prepared from the carbonated test specimen and examined under a polarized-light microscope. Approximate locations of photographs presented below are shown in Fig. 21.

Photomicrograph #1 in Fig. 22 shows a highly carbonated cement paste as evident from the strong birefringence of the ground mass. A close-up of a section in photomicrograph #1 (Fig. 23) shows reaction rims of calcite around silicate grains, as well as a highly carbonated cement paste. Photomicrographs 3 and 4 in Figs. 24 and 25 reveal presence of microfractures in cement paste between silicate grains filled in with calcitic material. Under crossed nicols, carbonate reaction rims surrounding silicate grains are quite evident (Fig. 25). Compared to photomicrographs in Figs. 22 and 23, Figs. 24 and 25 indicate that the cement paste appears to be relatively less carbonated. The photomicrograph (#5) in Fig. 26 shows no evidence of carbonation of cement paste, although carbonate reaction rims around silicate grains still persist. With increasing distance from the specimen interior towards the periphery, the cement paste has a granular, mottled texture, completely devoid of any carbonation alteration features (photomicrograph #6, Fig. 27), similar to the textural features of non-carbonated material (Fig. 28). Photomicrograph #7 in Fig. 29 reveals the presence of a narrow, well-defined carbonation zone, induced as a result of reaction with atmospheric CO_2, located at the periphery of the grout specimen.

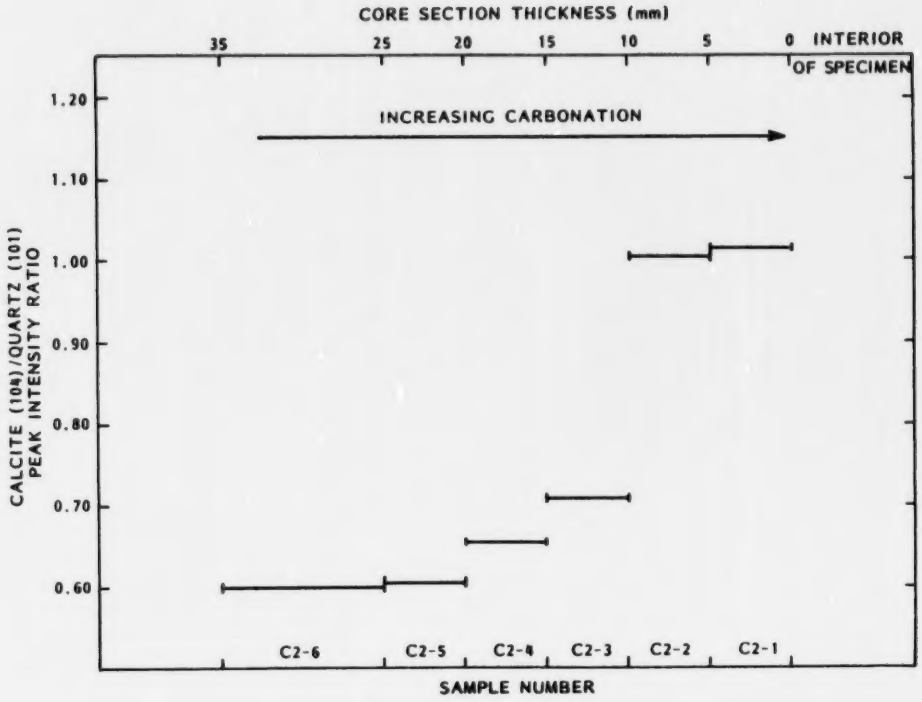

Figure 19. Calcite/quartz peak intensity ratios as a function of increasing distance from specimen interior of carbonated material.

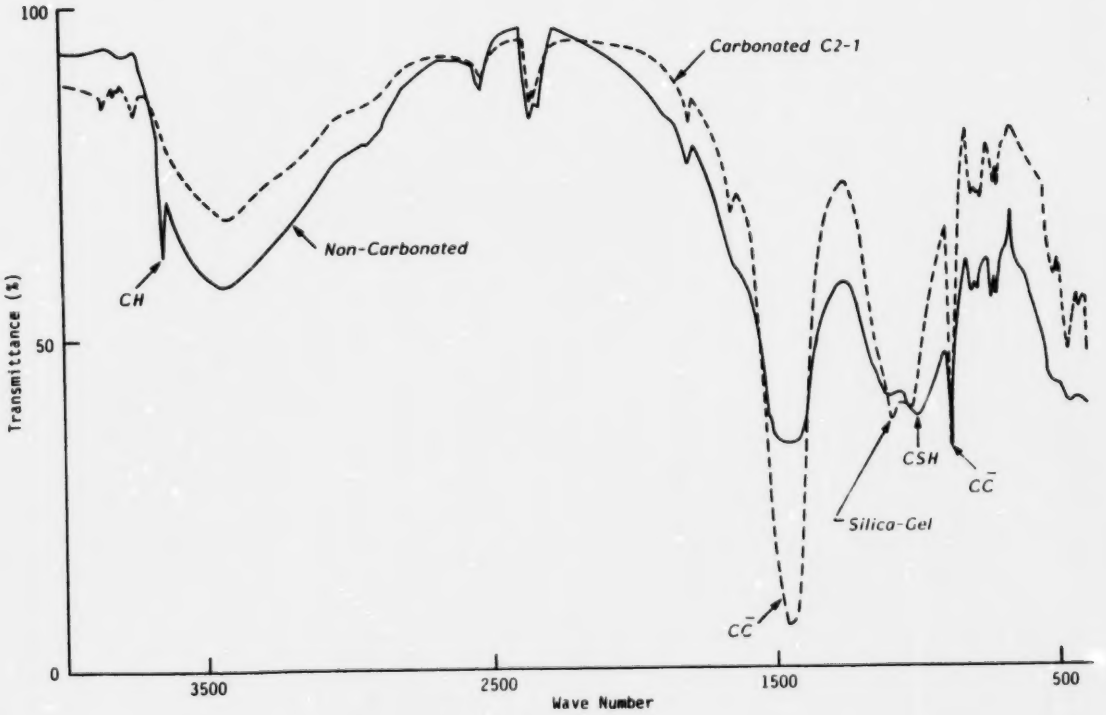

Figure 20. Infra-red spectra of non-carbonated and carbonated test material.

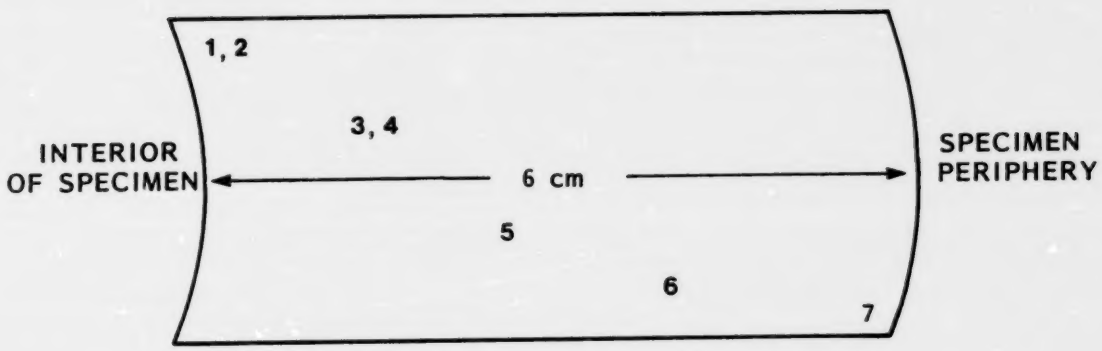

Figure 21. Numbers indicate approximate locations of areas photographed under plane-polarized light and crossed nicols.

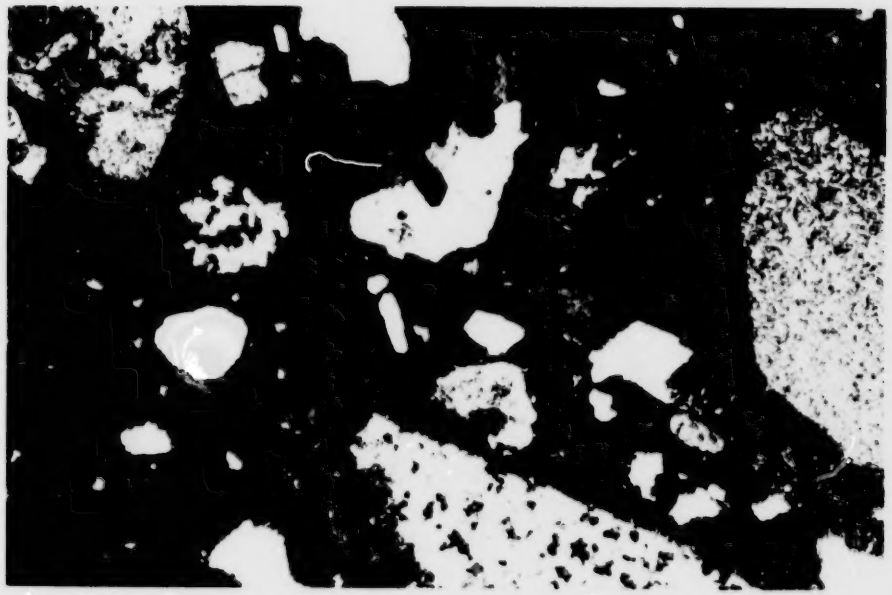

Figure 22. Photomicrograph (#1) showing a highly carbonated paste (crossed nicols, 10X).

Figure 23. Photomicrograph (#2) is a close-up of photomicrograph (#1) showing reaction rims of calcitic material around silicate grains, as well as a highly carbonated cement paste (crossed nicols, 40X).

Figure 24. Photomicrograph (#3) showing microcracks present in cement paste between mineral grains (plane-polarized light, 40X).

Figure 25. Photomicrograph (#4) same as photomicrograph (#3) showing microcracks filled in with highly birefringent calcitic material, as well as reaction rims around silicate grains and a relatively less carbonated cement paste (crossed nicols, 40X).

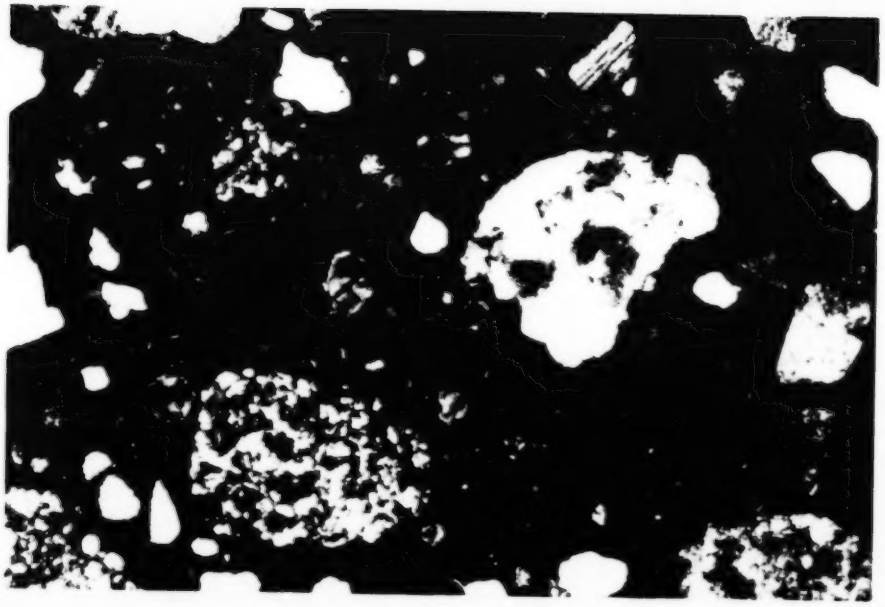

Figure 26. Photomicrograph (#5) showing a non-carbonated cement paste, but reaction rims around silicate grains persist (crossed nicols, 10X).

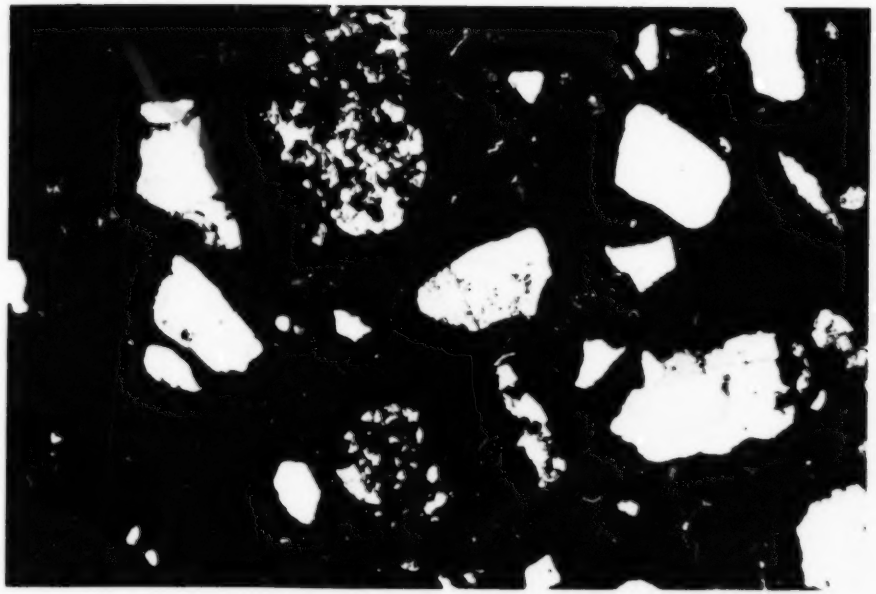

Figure 27. Photomicrograph (#6) showing cement paste with a granular, mottled texture, completely devoid of any carbonation features (crossed nicols, 10X).

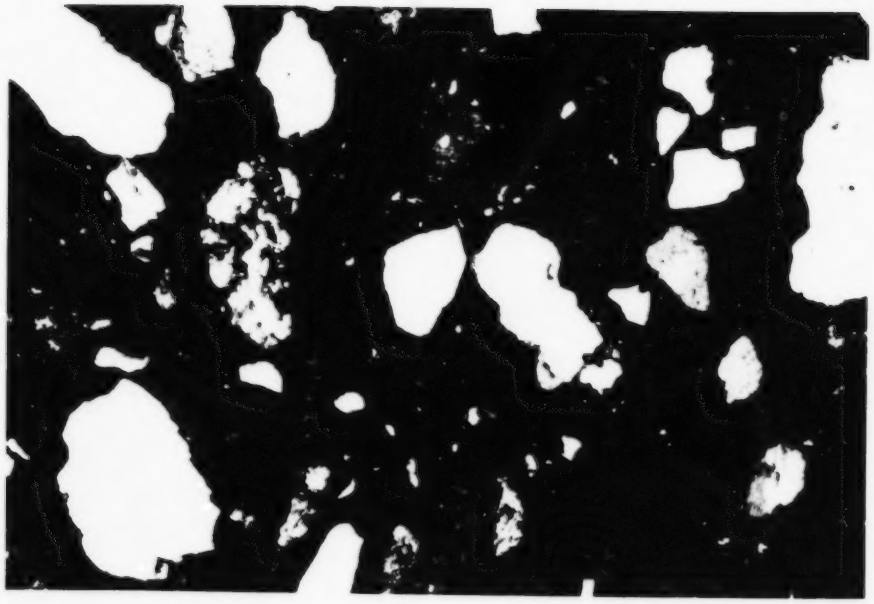

Figure 28. Photomicrograph of non-carbonated grout showing cement paste with a granular texture and lack of carbonation features (crossed nicols, 10X).

Figure 29. Photomicrograph (#7) showing a distinct carbonation zone at the outer edge of the specimen (crossed nicols, 10X).

Based on microscopic examination of the carbonated grout, it appears that the most intensely carbonated region of the specimen is represented by a 2 cm thick zone around the specimen cavity, although some carbonation features are still evident at a distance of ~3 cm. The observed changes in material properties also indicate the carbonation front to extend to a distance of ~3 cm from the specimen cavity.

3.3 Carbonation Mechanisms and C-14 Mobility

It is well-known that concrete, because of its highly alkaline character, undergoes carbonation by direct reaction with carbon dioxide as depicted by the following reactions.

$$Ca(OH)_2 + CO_2 \longrightarrow CaCO_3 + H_2O \quad (1)$$

$$\text{Ca-silicate hydrate} + CO_2 \longrightarrow CaCO_3 + \text{amorphous silica} + H_2O \quad (2)$$

Both carbonation reactions produce water.

In this particular study, the carbonation-induced phase changes observed in the test material appear to follow the two carbonation reactions. As discussed in the previous section (3.2.4), complete disappearance of portlandite and significant increase in calcite was observed following carbonation of test material. Microscopic examination also revealed a highly carbonated cement paste. Infra-red analysis indicates formation of silica gel at the expense of calcium silicate hydrate upon carbonation. This is also supported by the disappearance of the weak 11Å tobermorite peak upon carbonation of test material. Furthermore, photomicrographs reveal the presence of calcitic reaction rims around silicate grains. The observed phase changes due to carbonation result in a significant change in the character of the cement paste which, in turn, has a direct bearing on C-14 mobility.

Since the carbonation process involves diffusion of CO_2 in concrete, the material permeability and pore structure are important characteristics controlling C-14 mobility. Moreover, the changes induced in these characteristics, as a result of carbonation, will be equally important.

Our work shows that the test material, when subjected to successive carbonations, exhibits a progressive decrease in gas permeability. The carbonation reactions are also accompanied by production of water. This was evident from high humidity values, approaching saturation, during carbonation. Higher moisture content will tend to reduce gas diffusivity which, in turn, will impede diffusion of CO_2. Furthermore, the carbon dioxide will dissolve in any moisture present to form carbonic acid, which is normally more reactive with grout. However, the degree of saturation is important in that carbonation is reported to be minimal at a relative humidity of 100%.

As discussed in previous sections, this study has also demonstrated that carbonation of test material is also accompanied by significant reductions in material permeability, porosity, and pore size. All these changes in material

properties will directly affect C-14 mobility, in that, its diffusion in the porous matrix will be considerably impeded. This is clearly reflected in both carbon dioxide and nitrogen permeability tests performed in this study. Since the test material serves as an infinite sink for CO_2, we do not believe the availability of reaction sites to be rate-controlling in carbon dioxide reaction with grout. Our work indicates that it is the material properties such as permeability, porosity, pore size, as well as moisture content, and the changes induced in these properties as a result of carbonation, that will affect CO_2 diffusion and hence C-14 mobility in grout materials.

3.4 Effects of Carbonation on Radionuclide Attenuation and Water Ingress Properties

Although from a geochemical point of view the grout test material exhibits high reactivity for CO_2 thus having the potential to serve as an effective sink for radiocarbon escaping from a waste package, we must also understand the consequences of the induced carbonation on material properties relevant to backfill performance requirements.

An important consequence of carbonation is the clogging of pores by authigenic carbonate material as evidenced by systematic reductions in average pore size, porosity and permeability with increasing degree of carbonation (Fig. 30).

This is also reflected in textural changes observed in carbonated cement paste, indicating filling up of pores in the groundmass by fine-grained, calcitic material. Even the microcracks present in the carbonated cement paste, most probably induced as a result of carbonation, are filled in with highly birefringent carbonate material. Therefore, in qualitative terms, carbonation-induced changes in material properties are likely to have a significant effect on hydrologic properties, in particular, the water ingress properties of backfill materials in that reduced permeability will serve to control water ingress into the disposal system.

The carbonation-induced changes also appear to have a beneficial effect on radionuclide transport properties. Firstly, transport of the conservative radionuclides, such as tritium, into the environment will be attenuated because of significant reductions in porosity and permeability, accompanied by a corresponding increase in tortuousity. More importantly, filling up of pore space in carbonated cement paste by fine-grained, carbonate material, results in a significant increase in the reactive surface area of the test material. The more surface area there is available for reaction, the more the reactive radionuclide will be sorbed and retarded, relative to a conservative radionuclide. Fig. 31 shows enhanced Cs-137 sorption on higher specific surface area materials, representing increasing degree of material carbonation.

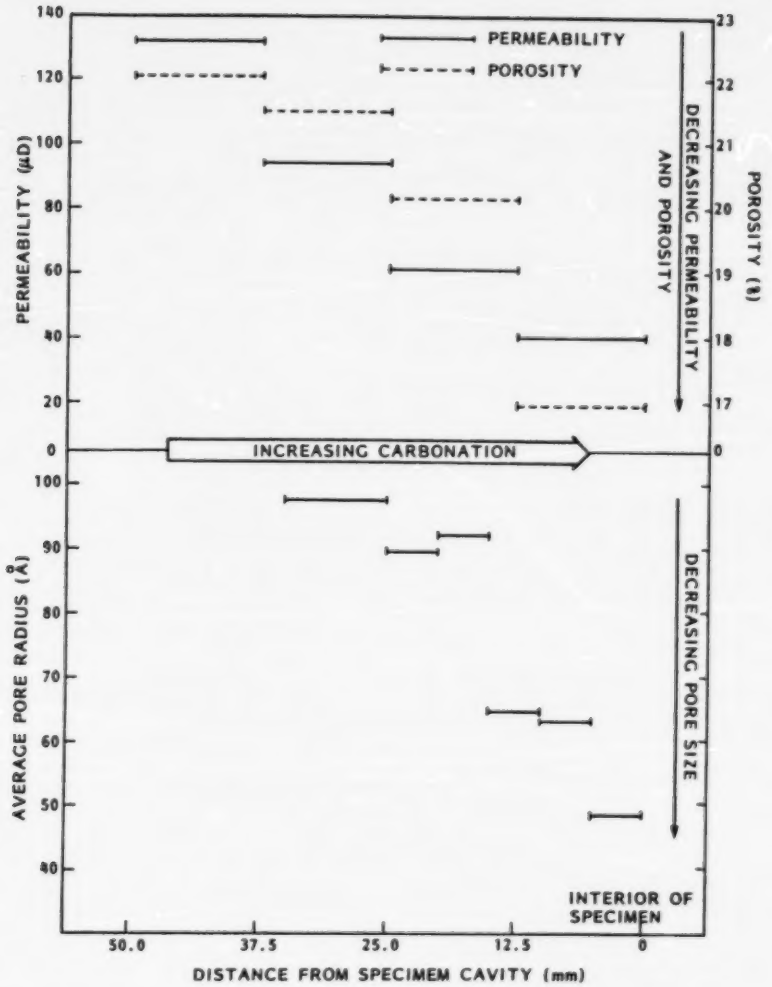

Figure 30. Decreasing permeability, porosity, and pore size with increasing degree of carbonation.

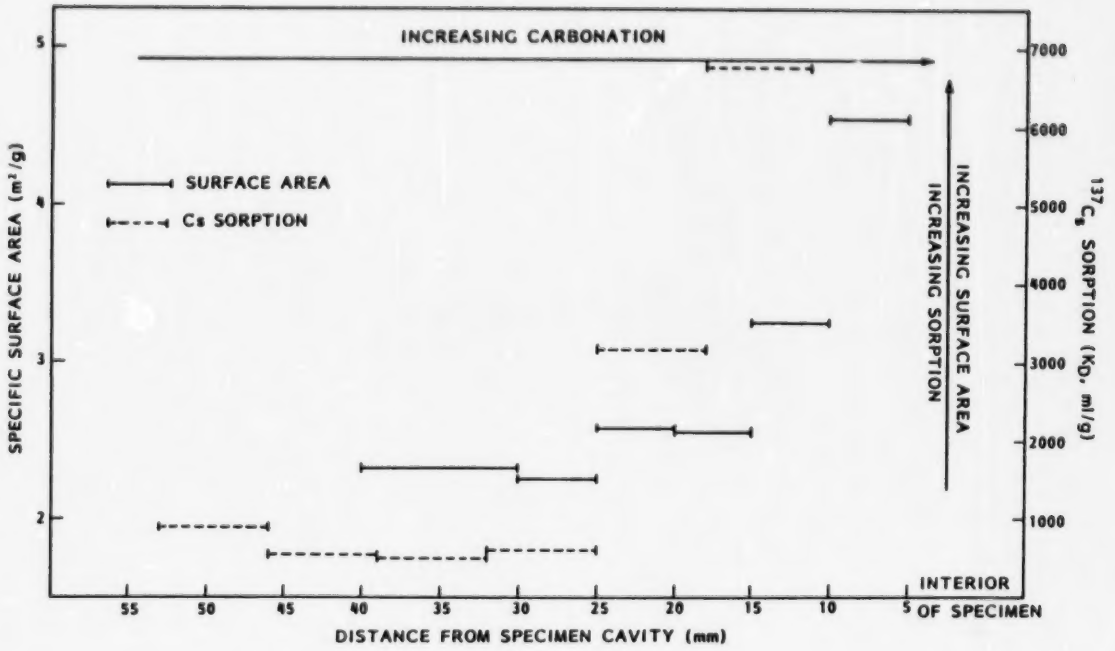

Figure 31. Increasing surface area and Cs sorption with increasing degree of carbonation.

4.0 CONCLUSIONS

Although preliminary at this stage, laboratory carbonation and permeability tests performed on a grout mix developed at Ontario Hydro indicate that cement-based materials have a high reactivity for CO_2, yielding carbonation products which have the potential to immobilize radiocarbon.

Nitrogen repeat tests demonstrate that the test material, when subjected to successive carbonations, exhibits a progressive decrease in gas permeability with increasing degree of carbonation.

Some of the important carbonation-induced changes in material properties include, with increasing degree of carbonation, a progressive reduction in permeability, porosity, and pore size, and a systematic increase in specific surface area.

The observed changes due to carbonation appear to have a beneficial effect on the radionuclide transport and water ingress properties of cement-based materials. Reduced permeability and porosity will tend to further minimize water ingress into the disposal system. Reduced water flow will also impede transport of radionuclides escaping from the waste package. Enhanced Cs-137 sorption on higher surface area carbonated material indicates that cement-based backfill, following carbonation, will serve as a more effective sink for reactive radionuclides.

Since the carbonation of grout is primarily a diffusion-controlled process, C-14 mobility would be considerably reduced with increasing degree of carbonation because of the observed reductions in permeability, porosity, and pore size.

Further work will concentrate on evaluation of other grout and concrete mixes developed at Ontario Hydro as potential backfilling materials. An important part of this work is to evaluate the reactivity of candidate materials for aqueous C-14, present as carbonate/bicarbonate, paying particular attention to the nature and extent of immobilization, and subsequent remobilization, if any, of C-14 in carbonated cement-based backfill materials.

5.0 ACKNOWLEDGEMENTS

The authors would like to acknowledge the assistance of M. Everitt for microscopic analysis of test specimens and D. Wilmot for carrying out radionuclide sorption tests.

Approved by:

for T.W. Klym
Manager
Civil Research Department

Reviewed by:

A.T. Jakubick
A/Supervising Engineer
Rock Sciences Section

RD/RK:cm

Submitted by:

R. Dayal
Senior Geochemist
Rock Sciences Section

R. Klein
Hydrogeology Technician
Rock Sciences Section

REFERENCES

Dayal, R. "Evaluation of Backfill Materials for Reactor Waste Disposal." Ontario Hydro Research Division Report, 86-348-K, 1986a.

Dayal, R. "Waste-Water Interactions and their Relevance to Nuclear Waste Disposal." Presented at the Fifth International Symposium on Water-Rock Interaction, Reykjavik, Iceland, 1986b.

Deans, J.J. "Evaluation of Superplasticized Concrete for the Low-Level and Medium-Level Waste Storage Test Facility." Ontario Hydro Research Division Report, S84-33-H, 1984.

Figg, J.W. "Methods of Measuring the Air and Water Permeability of Concrete." Magazine of Concrete Research, 25, 1973.

Jakubick, A.T., and Klein, R. "Multiparameter Testing of Permeability by the Transient Vacuum Technique." In Coupled Processes Associated with Nuclear Waste Repositories, Academic Press, 1987.

Loughborough, M.T. "Permeability of Concrete to Air." Ontario Hydro Research Report Quarterly, First Quarter, 1966.

Martin, G.R. "A Method for Determining the Relative Permeability of Concrete Using Gas." Magazine of Concrete Research, 38, 1986.

Moddle, P., Reardon, E.J., and Jakubick, A.T. "Carbon Dioxide Isolation Efficiency of Cementitious Grout." Presented at the Second International Conference on Radioactive Waste Management, Winnipeg, Manitoba, Canada, 1986.

Reardon, E.J. "Uptake of CO_2 in Reactor Waste Grout." Semi-Annual Progress Report, University of Waterloo, 1986.

DISTRIBUTION

Dr. D. Mills	Director of Research
Mr. H.N. Isaac	Design & Development-Gen, H11G27
Mr. B.P. Dalziel	Design & Development-Gen, H11D17
Mr. P.J. Armstrong	Design & Development-Gen, H11G20
Dr. S.J. Naqvi	Design & Development-Gen, H11D18
Dr. P.K.M. Rao	Design & Development-Gen, H11D2
Mr. K.J. Donnelly	Design & Development-Gen, H11F24
Dr. J. Freire-Canosa	Design & Development-Gen, H11E17
Dr. C.F. Lee	Design & Development-Gen, H18A23
Dr. R. Glass	Chemical Research
Dr. T.W. Klym	Civil Research
Dr. A.T. Jakubick	Civil Research
Mr. T.J. Carmichael	Civil Research
Mr. G.S. Kellay	Civil Research
Mr. J.J. Deans	Civil Research
Dr. R. Dayal (6)	Civil Research

Public Reference Centre
Editorial Section (2)
Office Copies (3)
Extra Copies (3)
Section File, KR258